

Variability of Monthly-Averaged Surface and 850 mb Winds at Tropical Pacific Islands

D. E. HARRISON

Center for Meteorology and Physical Oceanography, Massachusetts Institute of Technology, Cambridge, MA 02139 and Pacific Marine Environmental Laboratory/NOAA, Seattle, WA 98105

D. S. GUTZLER*

Center for Meteorology and Physical Oceanography, Massachusetts Institute of Technology, Cambridge, MA 02139

(Manuscript received 9 April 1985, in final form 8 July 1985)

ABSTRACT

We examine the variability of monthly mean winds at 850 mb and the surface from five island stations in the tropical western Pacific Ocean. Climatological winds and (850 mb–surface) wind shear are evaluated and used to construct time series of monthly mean wind and shear anomalies. Wind variance at 850 mb tends to be substantially greater than at the surface, and large temporal variations in shear are found. Prominent anomalies are associated with El Niño–Southern Oscillation periods. Composite El Niño event anomalies are examined; it is found that the westerly wind anomalies associated with warm central Pacific sea surface temperatures are stronger at 850 mb than at the surface, and that the anomalous (850 mb–surface) shears are as large as the surface wind anomalies themselves.

Several simple techniques are described to investigate the feasibility of estimating surface wind anomalies from 850 mb wind anomalies. Because strong correlations exist between the zonal winds at these levels, zonal estimate errors can be reduced to $\approx 0.5 \text{ m s}^{-1}$ if known shear statistics are included in the estimate algorithm. Estimates which extrapolate cloud level wind anomalies to the surface using only climatological shear are shown to produce much greater surface wind errors. If these results are representative and if accurate monthly mean winds at 850 mb can be obtained from cloud motion vectors, then very useful low-frequency surface wind fields can be derived from cloud motion data.

1. Introduction

The present interest in the variability of tropical atmospheric winds and the coupled ocean-atmosphere phenomenon of the El Niño–Southern Oscillation (ENSO) has led to increased study of winds at low levels in the tropics. Data generally available are: low-level cloud motion vectors (CMVs) which are typically assigned a nominal height of 850 mb in operational processing, and ship reports, island observations and buoy wind recorder data from very near the surface. The dataset for each level has limitations concerning data coverage in space and time, duration of records, and/or data quality.

Over the tropical Pacific, the two sets have often offered quite complementary spatial coverage, and efforts have been made to combine them (Sadler and Kilonsky, 1981, hereafter referred to as SK). Over the past few years, efforts to provide CMV data have been made by the European community and the Japanese and Indian governments. Global coverage is often available at present, but CMV data are obtained with different techniques and serious intercomparison remains to be done. Harrison (1984) provides a brief

survey of many of the issues pertinent to the use of the various types of data.

A crucial issue concerns how to adjust the cloud motion data to an appropriate near-surface level. Sadler and Kilonsky have used a monthly mean shear field constructed as the difference between climatological monthly mean CMV winds based on about seven years of data, and climatological monthly mean surface winds based on about 25 years of ship reports (Wyrski and Meyers, 1975). For a particular monthly mean CMV field, the climatological shear field is subtracted to produce a first-guess surface wind field, which is then blended subjectively with the available ship, island and buoy data into a surface wind field. Wylie and Hinton (1982) have described efforts to use a different type of empirical shear adjustment, which depends upon observed shear values for winds from different directions, evaluated region by region over the Indian Ocean during FGGE. Only the SK approach is in use in an ongoing basis.

Because the CMV dataset often provides spatial coverage and data density far superior to that available from the surface dataset, there is much interest in developing the best possible shear adjustment procedure (e.g., see WCP, 1983). For short time scales (days and less), it is well established that no systematic shear relationship exists between 850 mb and the surface (e.g., Kanton and Cole, 1980). But at lower frequencies the

* Present affiliation: CIRES, University of Colorado, Boulder, CO 80309.

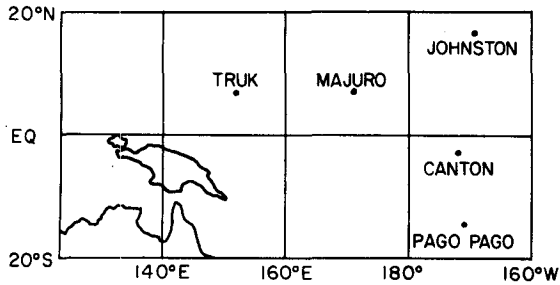


FIG. 1. Locations of the five Western Pacific islands considered in this study.

situation improves markedly, and SK have produced useful monthly mean fields. However, the tropical Pacific undergoes dramatic changes during ENSO periods, during which the utility of a climatological shear relationship is not obvious. For instance, should a shear value largely based on a prevailing easterly trade wind environment be expected to apply during periods of light easterlies to moderate westerlies?

As part of an ongoing study of the vertical and horizontal structure of low-frequency variability of tropical winds, we have used multi-year time series of monthly mean winds at 850 mb and at the surface at five islands in the central and western tropical Pacific (Fig. 1) to examine some of these issues. The rawinsonde observations at 850 mb will not necessarily be identical to CMV winds for the same time and place; there are various reasons why the two should differ in general and can differ greatly. Any results based on the 850 mb winds will probably represent "best case" results possible for CMV winds. Unfortunately, CMV winds generally are not available around these islands, because the GOES-W satellite which is the basis for the CMV data does not provide coverage this far west in the Pacific.

First we present the monthly mean seasonal cycles at the surface and at 850 mb for these islands, and summarize the seasonal variation of vertical shear. Next, the interannual variability is briefly summarized and the variance at 850 mb is shown to be much greater than at the surface.

We then examine the least-square optimum bilinear regression between 850 mb and surface winds (and other linear regressions), and show that it is crucial to know the ratio of the variances at the two levels in order to obtain a good surface zonal wind estimate. The surface wind anomalies are then estimated from the 850 mb winds using four different procedures, in-

cluding that of SK. The three others presented here produce much better estimates. Furthermore, we show that the regression coefficients for the zonal wind at each island are quite consistent, allowing us to formulate a simple, general adjustment scheme which works nearly as well as the statistically optimal parameterizations.

2. Data

Table 1 summarizes the time series that will be used in this work. The 850 mb monthly means are taken from *Monthly Climatic Data for the World*, archived on tape at the National Center for Atmospheric Research. The surface monthly means were constructed from tapes of individual observations in the National Climatic Data Center TDF-13 file. The surface data, in somewhat different form, have been described by Luther and Harrison (1984).

Gaps exist in the data records at Majuro, Canton, and Johnston, as can be seen by comparing the record length and period of record in Table 1. These gaps are due to missing or suspicious data in the upper air records. They occur early in the period at Majuro and Canton, in April 1969 at Johnston, and from November 1967 through November 1969 at Majuro. In addition, the period of record prior to January 1964 at Truk was neglected because the surface wind record contained a suspicious discontinuity at that point (Luther and Harrison, 1984).

The shortest time series is that at Canton, for which approximately ten years of (noncontinuous) data are used. Each estimate of the monthly climatological surface and 850 mb winds is based on at least nine samples. Elsewhere, the monthly climatological estimates are typically based on 12–18 samples.

3. The climatological cycle of monthly mean wind and shear

Figure 2a shows the climatological monthly mean 850 mb vector winds at the islands, plotted bimonthly. The zonal wind is easterly at all locations in every month, and is almost always stronger than the meridional wind. The meridional wind is less than 2 m s^{-1} , except early in the year at Pago Pago. The change through the year is greatest at Truk, where the magnitude of the vector wind varies between 1 and 8 m s^{-1} ; at the other islands the range is typically $3\text{--}5 \text{ m s}^{-1}$. Typical bimonth-to-bimonth vector magnitude changes are $1\text{--}2 \text{ m s}^{-1}$ except sometimes late in the

TABLE 1. Data characteristics for the five island wind stations used in this study.

	Truk	Majuro	Canton	Pago Pago	Johnston
Latitude, longitude	7.5°N, 151.9°E	7.1°N, 171.4°E	2.8°S, 171.4°W	14.3°S, 170.6°W	17.0°N, 169.5°W
Period of record	Jan 64–Dec 78	Jan 59–Dec 78	Jan 57–Aug 68	Apr 66–Dec 78	Nov 62–Dec 78
Record length (months)	180	210	121	153	193

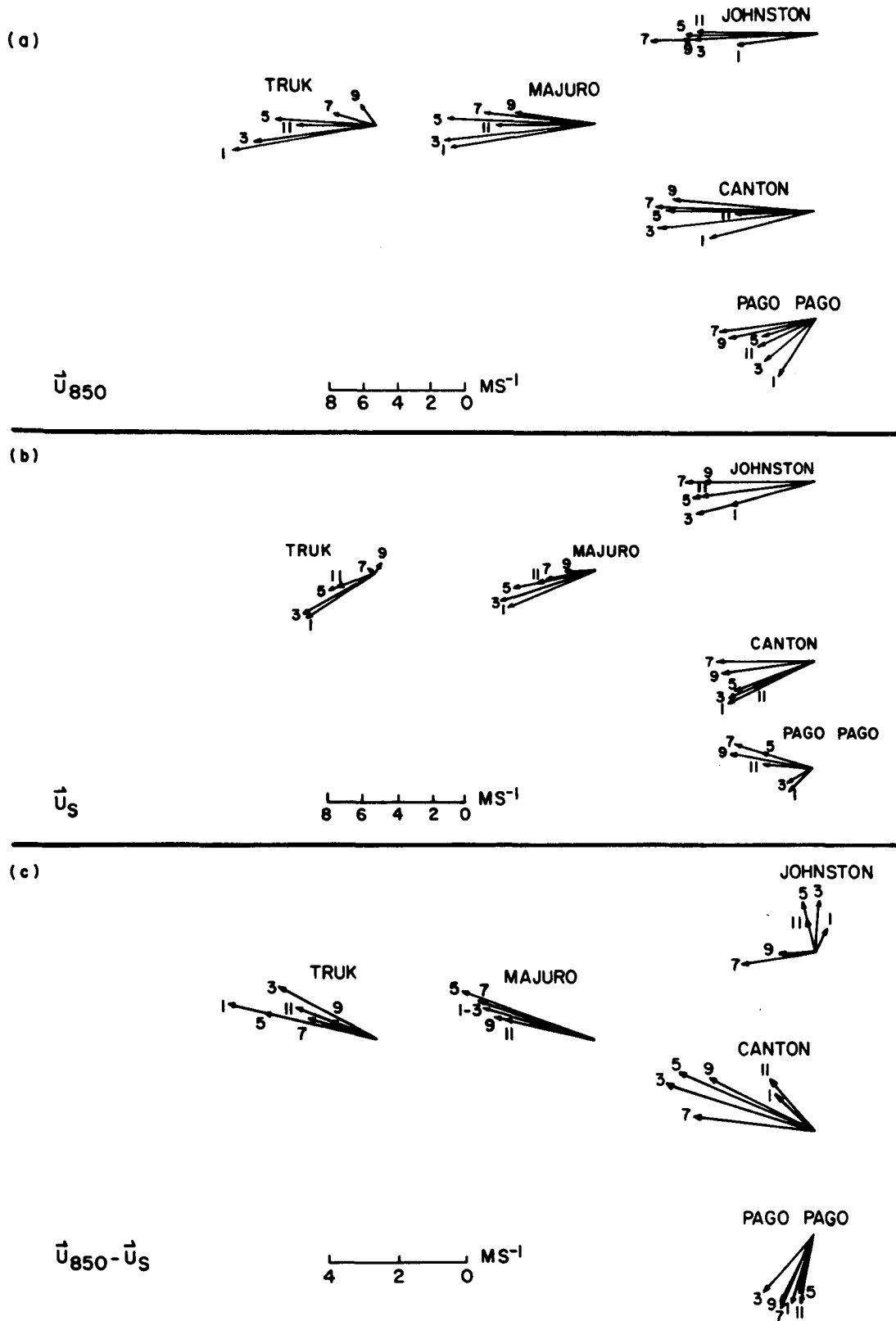


FIG. 2. (a) Climatological mean 850 mb wind vectors for the months of January, March, May, July, September, and November (labeled 1, 3, 5, 7, 9, 11, respectively). (b) As in (a) but for surface wind vectors. (c) As in (a) but for (850 mb-surface) shear vectors.

year, when they can be $4\text{--}5 \text{ m s}^{-1}$ as at Truk and Canton.

Figure 2b presents the surface winds in analogous fashion. The climatological surface winds shown here agree quite closely with the ship data compiled by Wyrski and Meyers (1975), despite the differences in data source and periods of record. Note that the mean winds are generally weaker and less zonal at the surface than at 850 mb; the typical annual range is also somewhat smaller. Maximum bimonthly changes are similar to those at 850 mb.

The climatological vector wind shears between 850 mb and the surface are given in Fig. 2c. They are quite different from island to island. At Pago Pago the shear vectors differ by less than 1 m s^{-1} from bimonth to bimonth. At Truk, Johnston, and Canton the shear varies by as much as 4 m s^{-1} throughout the year, and up to 2 m s^{-1} between bimonths. At Truk and Majuro the shear vectors are nearly colinear throughout the year (angular difference is less than 20°); they vary over about 30° at Pago Pago, 45° at Canton and 120° at Johnston.

Another aspect of the shear is the angle between the 850 mb and surface wind vectors. The climatological shear angle entered in Table 2 was determined by averaging the angular differences between the bimonthly surface and 850 mb wind vectors shown in Fig. 2 for each island. Clockwise turning from the surface to the 850 mb level (i.e. anticyclonic turning in the Northern Hemisphere and cyclonic turning in the Southern Hemisphere) was defined to be positive, and a turning angle was calculated only if both surface and 850 mb wind speeds were greater than 1.0 m s^{-1} .

Although the magnitude of the climatological turning angle varies widely from island to island, the signs are consistent with Ekman dynamics in the boundary layer, except at Canton. Month-to-month variability in the climatological turning angle (not presented) is typically about half the mean value at each island; the sign of the angle does not change at any particular island throughout the year.

Clearly, the space and time variation of the clima-

tological shear is substantial, and cannot generally be well approximated by any simple function of space or time. Such variations are plausible, because these islands exist in quite distinctly different tropical wind regimes, and no island is in the same sort of regime throughout the year.

4. Monthly mean wind variability

We shall concentrate on the anomalies, defined relative to the monthly mean climatological cycle. Figures 3–5 present vector time series of anomalous monthly mean wind at 850 mb, the surface, and the 850 mb–surface shear, respectively. Table 2 provides a statistical summary of these records.

From Fig. 3 and Table 2 it is clear that the dominant variability at 850 mb is in the zonal component; the ratios of standard deviations (σ_u/σ_v) at 850 mb range from 1.6 at Pago Pago to 4.1 at Canton, and the average ratio for all the islands is about 3 (Table 2). At the surface, the ratios of zonal to meridional standard deviation are smaller, ranging from 1.0 at Johnston to 1.5 at Majuro and Canton. The ratio of zonal standard deviation at the surface to that at 850 mb is quite constant, varying between 0.47 and 0.63. No similar constancy is found between meridional standard deviations.

The clearest signals at 850 mb are seen at Canton, where the monthly mean variability is spectrally “red”. Episodes of substantial duration of significant westerly anomaly are seen in late 1957–58, late 1963, and late 1965–66, which are El Niño periods. No periods of sustained westerly anomaly exist except during El Niño events. At Truk and Majuro the situation is less clear: sustained westerly anomalies are observed in 1963, 1972, 1976, and 1977 at Majuro, and in 1965, 1967, 1968, 1972, 1974, 1976, and 1977–78 at Truk. In addition, periods of sustained easterly anomalies are just as prevalent, but the magnitude of the anomalous easterlies is substantially less than the westerly anomalies associated with ENSO. No straightforward relationship is found at Pago Pago or Johnston, where the time series contain less persistence in general.

TABLE 2. Turning angle and wind statistics.

	Truk	Majuro	Canton	Pago Pago	Johnston
Turning angle					
climatological (850–surface)	22°	13°	16°	–24°	5°
anomalous (850–surface)	9°	5°	2°	–2°	11°
standard deviation	29°	28°	60°	29°	29°
Standard deviation of					
anomalous zonal wind					
} 850	2.4	1.9	2.5	1.7	2.0
} surface	1.1	0.9	1.4	1.1	1.3
anomalous meridional wind					
} 850	0.8	0.7	0.6	1.1	0.8
} surface	0.7	0.6	0.9	0.8	1.3
Correlation $r_u(u_s, u_8)$	0.90	0.86	0.77	0.70	0.87
Correlation $r_v(v_s, v_8)$	0.53	0.58	–0.01	0.68	0.61

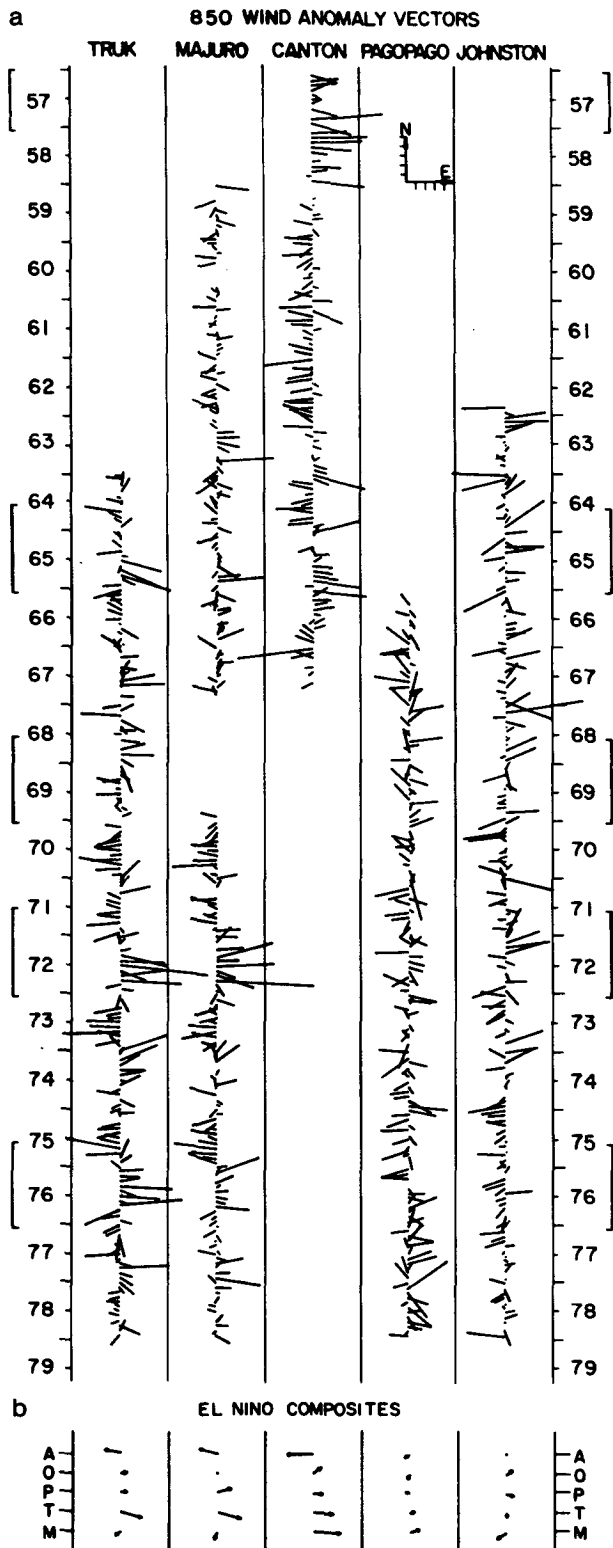


FIG. 3. (a) Time series of monthly mean anomalous 850 mb wind vectors (monthly mean 850 mb wind minus monthly climatology) for the five islands. Note the scale for u and v components in the column for Pago Pago: each tick mark represents 1 m s^{-1} . Vertical bars to left and right of the time series delineate El Niño events used

Luther and Harrison (1984) have discussed the changes in these surface wind records associated with El Niño events. A brief comparison of plotted surface anomalies (Fig. 4) with the 850 mb anomalies in Fig. 3 emphasizes the implications of the statistics displayed in Table 2: at the surface, the variability is generally less than at 850 mb and is more evenly distributed between the zonal and meridional components. Episodes of persistent zonal anomalies at the surface match up well with zonal anomalies at 850 mb. Persistent meridional anomalies are evident in the surface record as well—for example, a southerly anomaly at Pago Pago appears in late 1975 and persists through 1976, despite changes in sign of the zonal anomaly.

Shear anomalies (Fig. 5) are generally of the same magnitude as the surface anomalies. Hence, neglect of anomalies in the 850 mb–surface shear when estimating surface winds from CMV data will inevitably produce estimate errors comparable to the surface anomalies themselves.

An average turning angle for wind anomaly vectors was calculated, considering only months where both surface and 850 mb anomalous speeds exceeded 1.0 m s^{-1} (one-third to one-half of all months). As shown in Table 2, this average turning angle had the same sign as in climatology for each island, but individual values showed wide variability despite the rather stringent minimum wind speed criterion. These results indicate that there is little utility to the notion of a mean turning angle for the extrapolation of CMV data to the surface.

As an example of a well-known signal in the surface wind field, we examined the wind anomalies associated with the life cycle of the composite El Niño event as defined by Rasmusson and Carpenter (1982). Composite three-month average anomalies of 850 mb wind, surface wind, and (850–surface) shear for the five canonical event phases defined by Rasmusson and Carpenter are shown at the bottom of Figs. 3, 4 and 5, respectively. The composites are centered respectively on the September preceding each El Niño (the “Antecedent” phase), followed by the subsequent December (“Onset” phase), April (“Peak” phase), September (“Transition” phase), and January (“Mature” phase). The five El Niño events (1957, 1965, 1969, 1972, 1976) for which we have data are delineated by vertical bars in Figs. 3a, 4a and 5a.

Qualitatively, the composite surface anomalies depicted here are similar to the Rasmusson and Carpenter composites at all islands except Pago Pago, where the composite anomalies shown here have much smaller magnitudes than the strong southerly anomalies shown by Rasmusson and Carpenter. No consistent, quantitative relationship is evident between the surface and

for composite anomalies shown in (b). (b) Composite El Niño anomalies, representing three-month averages of Antecedent, Onset, Peak, Transition, and Mature phases, labeled A, O, P, T, and M, respectively (see text for details).

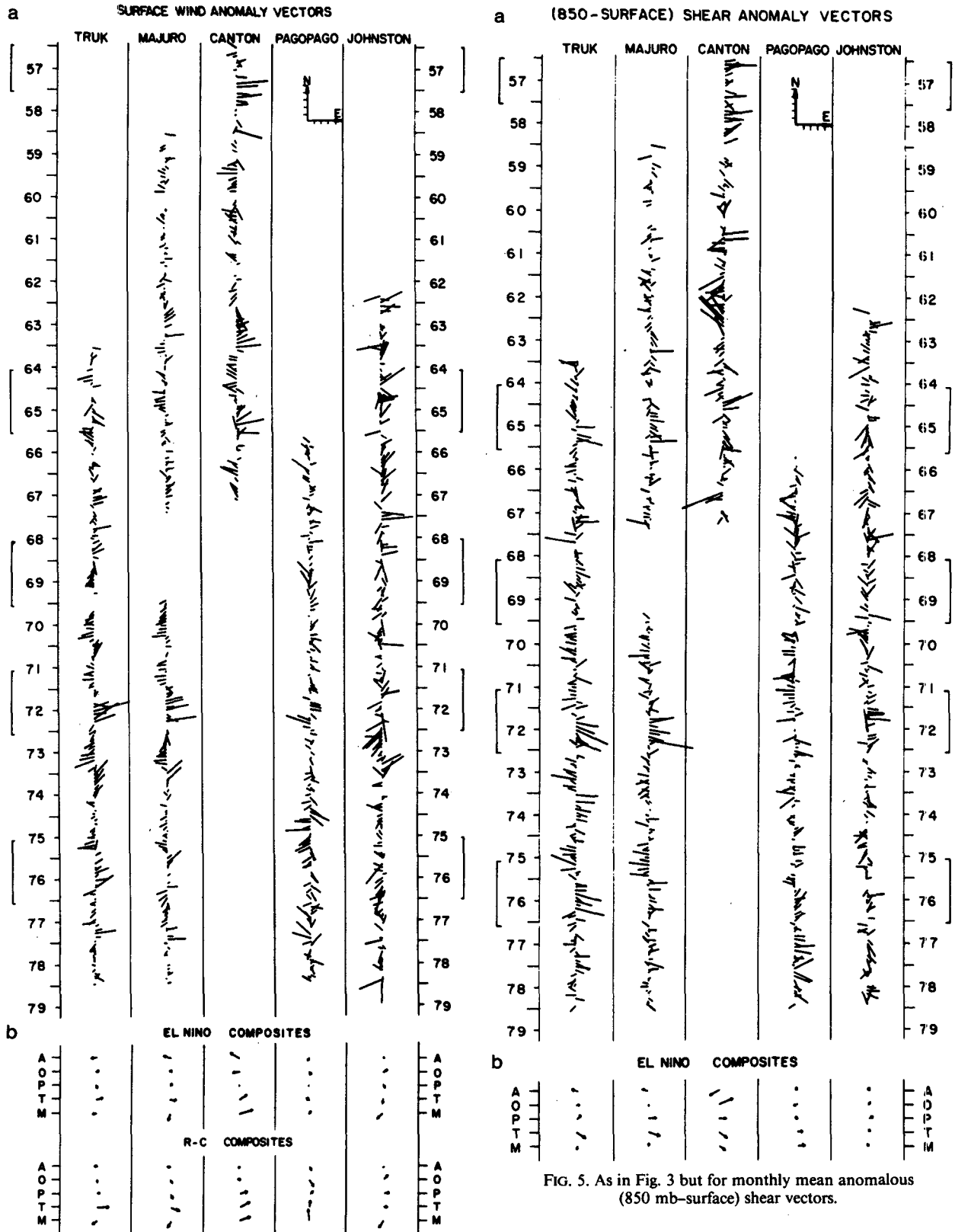


FIG. 4. (a, b) As in Fig. 3a, b but for monthly mean anomalous surface wind vectors. (c) Composite El Niño surface wind vectors taken from Rasmusson and Carpenter (1982) at gridpoints adjacent to the five islands studied here.

FIG. 5. As in Fig. 3 but for monthly mean anomalous (850 mb-surface) shear vectors.

850 mb vector anomalies. However, it is clear that the 850 mb anomalies are typically larger, particularly so for the Antecedent phase and for the largest anomalies. In other words, anomalous surface and 850 mb winds are associated with anomalous shear. A direct extrapolation of 850 mb wind anomalies to the surface using the climatological shear would systematically overestimate the true surface anomalies. Since the equatorial ocean-atmosphere system is quite sensitive to anomalous surface wind convergence, an "observed" surface wind field prepared with 850 mb level anomalies brought directly to the surface (as in SK) could lead to very misleading interpretations.

5. Estimating surface wind anomalies from 850 mb winds

In this section we consider how best to use information from 850 mb, just above the planetary boundary layer, to estimate the variation of surface wind anomalies. We use an elementary statistical approach and find substantial improvement over the method of SK.

First, consider a least-square bilinear regression

$$u'_{se} = a_u u'_8 + b_u v'_8 \tag{1a}$$

$$v'_{se} = a_v u'_8 + b_v v'_8. \tag{1b}$$

Here u'_{se} and v'_{se} are our estimates of surface zonal and meridional anomalous wind, u'_s and v'_s respectively, in terms of the known anomalies u'_8 and v'_8 at 850 mb. The constants are determined empirically and are presented in Table 3. It is found that a_u varies between 0.42 and 0.55 and is typically much larger than b_u . Because u'_8 typically dominates v'_8 it seems that u'_{se} is best determined primarily by u'_8 . Useful estimation of v'_s requires knowledge of both u'_8 and v'_8 , at least for Canton and Truk.

The bilinear regressions provide a very good estimate of u'_s , as shown in Table 4. The standard deviations of the time series of estimates are generally slightly less than the observations (cf. Table 2), but greater than

the root-mean-square errors. For example, at Majuro the time series of observed surface zonal wind has a standard deviation of 0.9 m s^{-1} . The bilinear estimate (1a) yields a time series with a standard deviation of 0.8 m s^{-1} , and rms errors of 0.4 m s^{-1} . Correlation coefficients between the estimated and observed zonal anomalies (not shown) range from 0.71 at Pago Pago to 0.91 at Truk. As suggested above, neglecting v'_8 in estimating u'_s has very little effect; estimate and error standard deviations for the linear parameterizations typically only vary by 0.1 m s^{-1} from the bilinear values.

To express this more precisely, if the meridional component is neglected, it is easily shown that the optimum (least-square) linear prediction of u'_s in terms of u'_8 has the form

$$u'_{se} = r_u \left[\frac{\sigma_{u(s)}}{\sigma_{u(8)}} \right] u'_8, \tag{2}$$

where r_u is the correlation coefficient between u'_s and u'_8 . The quantity on the right-hand side of (2) defines the regression coefficient a in Table 3; the corresponding quantity for meridional winds is the coefficient b . From Table 3, it can be seen that r_u is generally near 1 (i.e., u'_s and u'_8 are highly correlated), and $[\sigma_{u(s)}/\sigma_{u(8)}] \approx 0.5$, so that a varies only between 0.42 and 0.55 from island to island. Hence, a very good estimate of u'_s can be obtained from the simple formula

$$u'_{se} = 0.5u'_8. \tag{3}$$

Notice that the SK adjustment is equivalent to

$$u'_{se} = u'_8 \tag{4a}$$

$$v'_{se} = v'_8 \tag{4b}$$

so that we expect surface zonal wind anomaly estimates made this way to be too large by roughly a factor of two, at least for the area being considered here.

Comparisons of time series of the surface zonal wind estimate error, using (1a), (2), (3), and (4a) in Table 4 clearly illustrate these points. Figures 6 and 7 show time series of u'_{se} using (1a), (3), and (4a) for Majuro and Truk, respectively. The traces based on (1a) and (3) are quite similar, and the errors are typically 0.5 m s^{-1} or less. Errors tend to persist for the largest times during ENSO periods. The SK estimate (4a) produces much larger errors than either (1a) or (3).

Errors associated with the surface meridional component estimates are relatively larger. The standard deviations of the estimates are typically no larger than the error standard deviations, even for the bilinear regressions. At Canton, the surface meridional wind component is completely uncorrelated with the 850 mb wind (Table 2), so the estimates have no skill whatsoever. In general, the surface-850 mb coupling is much weaker for the meridional component. Coincidentally, the meridional analogue to (3)

TABLE 3. Empirical regression coefficients for (1) and (2) as follows.

	Truk	Majuro	Canton	Pago Pago	Johnston
(1) bilinear regression: $u'_{se} = a_u u'_8 + b_u v'_8$; $v'_{se} = a_v u'_8 + b_v v'_8$					
(2) linear regression: $u'_{se} = a u'_8$; $v'_{se} = b v'_8$					
(3) simplified parameterization: $u'_{se} = \frac{1}{2} u'_8$; $v'_{se} = \frac{1}{2} v'_8$					
(4) SK parameterization: $u'_{se} = u'_8$; $v'_{se} = v'_8$					
a_u	0.42	0.42	0.42	0.43	0.55
b_u	0.10	0.21	-0.10	-0.15	0.00
a_v	0.13	0.06	-0.01	-0.03	0.06
b_v	0.50	0.50	-0.02	0.52	0.92
a	0.42	0.42	0.42	0.44	0.55
b	0.49	0.51	-0.02	0.53	0.98

TABLE 4. Standard deviations of the time series of estimated surface wind anomalies $[(u'_{se})^2]^{1/2}$ and $(v'_{se})^2]^{1/2}$ and error standard deviations $\{[(u'_{se} - u'_s)^2]^{1/2}$ and $[(v'_{se} - v'_s)^2]^{1/2}\}$ for the parameterizations defined in Table 3.

		Truk	Majuro	Canton	Pago Pago	Johnston
Estimates						
Zonal wind	1	1.0	0.8	1.0	0.8	1.1
	2	1.0	0.8	1.0	0.7	1.1
	3	1.2	1.0	1.2	0.8	1.0
	4	2.4	1.9	2.5	1.7	2.0
Meridional wind	1	0.5	0.4	0.0	0.6	0.8
	2	0.4	0.4	0.0	0.6	0.8
	3	0.4	0.3	0.3	0.5	0.4
	4	0.8	0.7	0.6	1.1	0.8
Errors						
Zonal wind	1	0.5	0.4	0.9	0.7	0.6
	2	0.5	0.5	0.9	0.8	0.6
	3	0.5	0.5	0.9	0.8	0.6
	4	1.4	1.2	1.7	1.2	1.1
Meridional wind	1	0.5	0.5	0.9	0.6	1.0
	2	0.6	0.5	0.9	0.6	1.0
	3	0.6	0.5	0.9	0.6	1.1
	4	0.7	0.6	1.1	0.8	1.0

$$v'_{se} = 0.5v'_8 \quad (5)$$

works nearly as well as the bilinear fit (1b), but in this case the correlations r_v are smaller than r_u while the standard deviation ratios are more nearly 1, so when multiplied together the factor of 0.5 is preserved. That is, (5) can be used to extrapolate 850 mb wind anomalies to the surface with nearly as much skill as (1b), but the fraction of variance explained by either (1b) or (5) is small.

The significance of these results was tested by recalculating the regression coefficients separately for the first and second halves of each island's time series. Values of a_u and a for each half record at each island were within 10% of the values listed in Table 3 with the exception of Pago Pago, where a_u was calculated to be 0.38 and 0.52 for the first and second halves, respectively. Values of b_u were consistently small except for the second half record at Pago Pago, for which it was -0.29. The meridional coefficients a_v , b_v , and b were much less reproducible; in some cases even the signs of these coefficients changed from one-half of the record to the other.

6. Concluding remarks

We have shown that very strong correlations exist between monthly mean zonal wind anomalies at 850 mb and those at the surface in the central and western tropical Pacific. A bilinear regression between surface and 850 mb winds leads to correlations between zonal surface wind anomaly estimates and true zonal surface

wind anomalies of about 0.8 and error standard deviations of 0.5 to 0.9 $m s^{-1}$. For surface zonal wind anomaly estimates it is satisfactory to neglect the meridional wind anomaly entirely and to take

$$u'_{se} = 0.5u'_8.$$

The SK procedure appears to produce zonal wind errors roughly twice as large as can be obtained using this expression.

The bilinear estimate for v'_{se} is somewhat superior to any simple relationship like (5), but no estimate examined here does as well for v'_{se} as is possible for u'_{se} . Still, an accurate estimate of only the zonal wind is valuable, because much of the variance of surface winds is contained in the zonal component. The lack of skill in obtaining reliable meridional surface wind estimates implies that surface convergence fields may be suspect, however.

The apparent universality of the factor of 0.5 in (3) is a surprising outcome of this study. Does it also hold for other locations over the tropical ocean? No simple physical justification for this value or for its generality is evident. However, considering that these five islands receive widely varying amounts of precipitation, and that the rainfall rate at each island has dramatic interannual and seasonal variability (particularly associated with ENSO), it seems unlikely that local convective activity is responsible. Should (3) prove to be a general result, it will pose an interesting result to be explained by tropical boundary layer theory.

However, simple schemes such as (3) only work

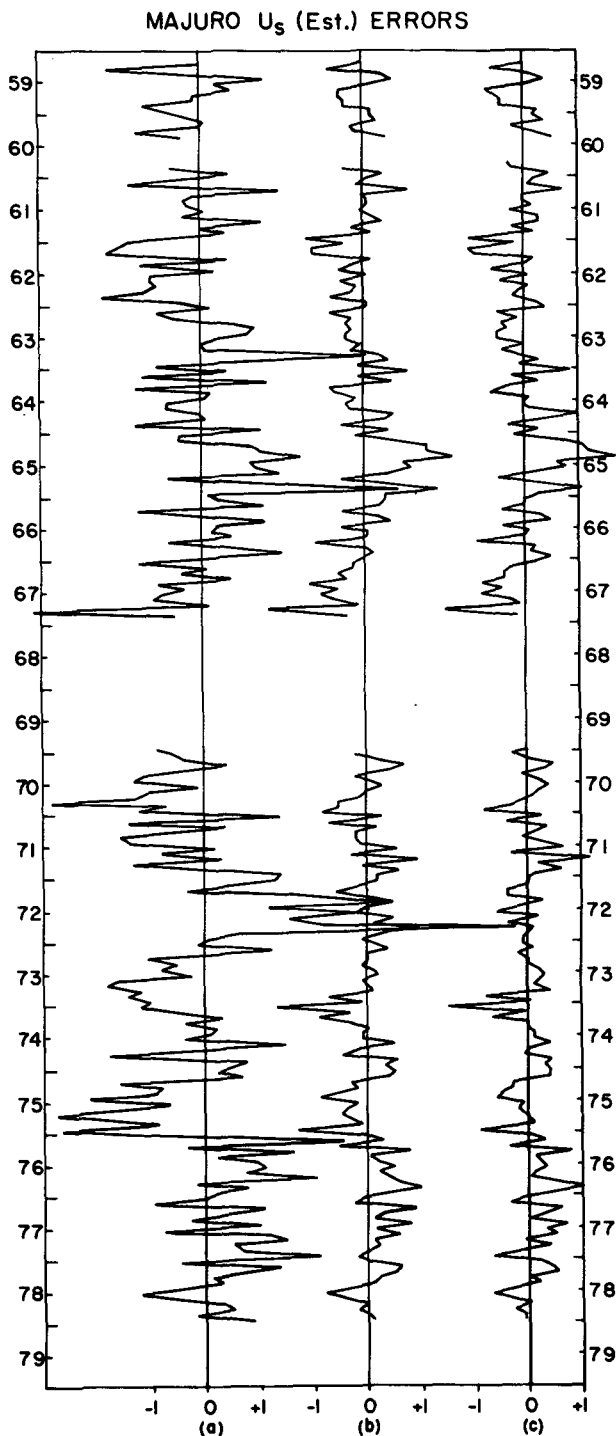


FIG. 6. Time series of zonal wind estimate errors ($u_{se} - u_s$) at Majuro for (a) Sadler and Kilonsky parameterization 4 in Table 3, (b) simplified parameterization 3 in Table 3 and (c) bilinear regression 1 in Table 3.

when applied to wind *anomalies* and not to the wind field itself. It is readily seen from Fig. 2 that the climatological shear varies from month to month and

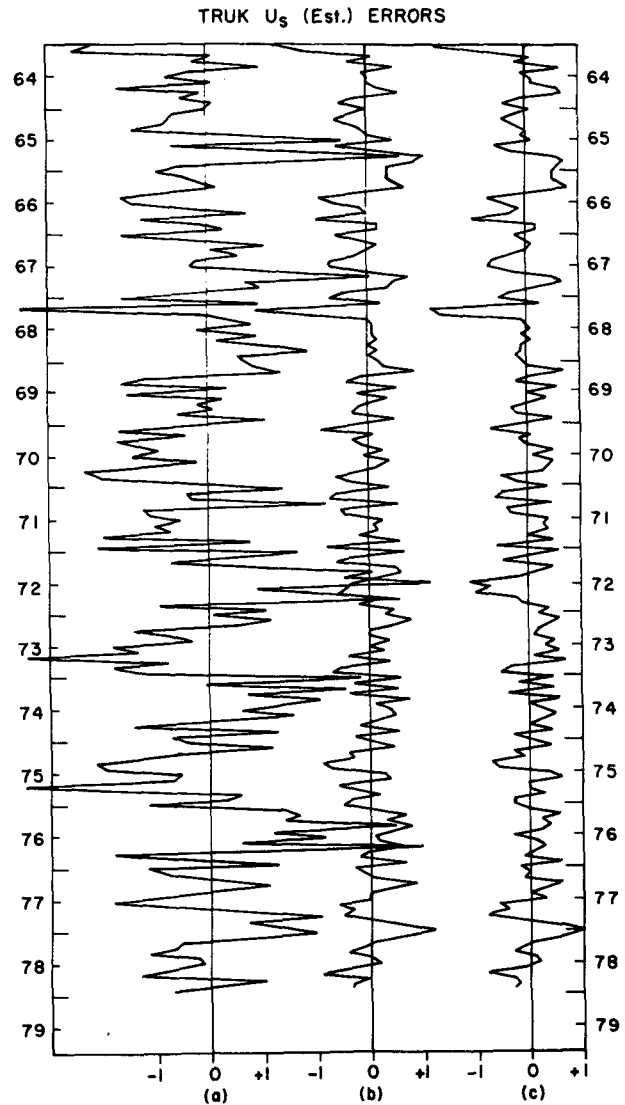


FIG. 7. As in Fig. 6 but for Truk.

from island to island, so that the climatological analogue of (3)

$$\bar{u}_s = 0.5\bar{u}_8$$

does not hold generally with any useful degree of accuracy.

We have seen that strongly anomalous periods tend to have strongly anomalous shear between 850 mb and the surface, as might have been anticipated. The SK adjustment scheme for cloud motion vectors will tend to produce the largest surface wind errors during these dynamically important periods. A very pleasing finding of this work is that surface errors based on the regressions presented are not significantly greater than normal during El Niño events.

To the extent that cloud motion vector anomalies reproduce 850 mb wind anomalies and also that (2) or (3) are applicable and the needed coefficients known, CMV anomaly data appear able to usefully augment other surface zonal wind anomaly data. But the SK procedure appears likely to lead to surface wind errors much larger than can be obtained using (2) or (3).

It is important to keep in perspective the limited spatial coverage of our data when attempting to generalize these results. The relevance of (3) to the remainder of the tropical Pacific is not known. However, it has been shown here to be useful for a wide range of meteorological environments and its apparent universality deserves to be examined further with other data.

This work does not begin to address other issues pertinent to a determination of how best to use CMV data to document surface wind variations. Obvious limitations include the use of monthly mean data, the lack of data between the surface and 850 mb, and the absence of contemporaneous surface data. There is a clear need for detailed comparison of individual and time-averaged CMV data and rawinsonde data. We hope that the international TOGA program may provide the impetus for further data collection and study on the many issues of relevance.

Acknowledgments. This work was supported by NSF Grant OCE83-01787 to M.I.T. and by TOGA and EPOCS Grants to P.M.E.L.

REFERENCES

- Harrison, D. E., 1984: Ocean surface wind stress. *Large-Scale Oceanographic Experiments and Satellites*, C. Gautier and M. Fieux, Eds., Reidel 99-115.
- Kantor, A. J., and A. E. Cole, 1980: Wind distributions and interlevel correlations, surface to 60 km. Air Force Geophysics Laboratory, Environ. Res. Paper No. 713, 115 pp. [AFGL-TR-80-0242].
- Luther, D. S., and D. E. Harrison, 1984: Observing long-period fluctuations of surface winds in the tropical Pacific: Initial results from island data. *Mon. Wea. Rev.*, **112**, 285-302.
- Rasmusson, E. M., and T. H. Carpenter, 1982: Variations in tropical sea surface temperature and surface wind fields associated with the Southern Oscillation/El Niño. *Mon. Wea. Rev.*, **110**, 354-384.
- Sadler, J. C., and B. J. Kilonsky, 1981: Tradewind monitoring using satellite observations. Rep. UHMET 81-01, Department of Meteorology, University of Hawaii, 23 pp.
- World Climate Program, 1983: Interim ocean surface wind data sets, No. 68. ICSU/WMO International TOGA Office, WMO Secretariat, Geneva, Switzerland.
- Wylie, D. P., and B. B. Hinton, 1982: The wind stress patterns over the Indian Ocean during the summer monsoon of 1979. *J. Phys. Ocean.*, **12**, 186-199.
- Wyrtki, K., and G. Meyers, 1975: The trade wind field over the Pacific Ocean, Part 1: The mean field and the mean annual variation. *Hawaii Institute of Geophysics, Rep. HIG-75-1*, 25 pp.